Sedimentology (2009) **56,** 873–892 doi: 10.1111/j.1365-3091.2008.01002.x

Environmental history of southern Patagonia unravelled by the seismic stratigraphy of Laguna Potrok Aike

FLAVIO S. ANSELMETTI*, DANIEL ARIZTEGUI†, MARC DE BATIST‡, A. CATALINA GEBHARDT§, TORSTEN HABERZETTL¶, FRANK NIESSEN§, CHRISTIAN OHLENDORF** and BERND ZOLITSCHKA**

**Eawag, Swiss Federal Institute of Aquatic Science and Technology, Department of Surface Waters, Überlandstrasse 133, CH-8600 Dübendorf, Switzerland (E-mail: flavio.anselmetti@eawag.ch)*

†*Section of Earth Sciences, University of Geneva, CH-1205 Geneva, Switzerland*

‡*Renard Centre of Marine Geology, Universiteit Gent, B-9000 Gent, Belgium*

§*Alfred-Wegener-Institut für Polar- und Meeresforschung (AWI), D-27570 Bremerhaven, Germany*

¶*ISMER, University of Québec, Rimouski, Québec, G5L 3A1, Canada*

***Institute of Geography, University of Bremen, D-28359 Bremen, Germany*

Associate Editor: Nick Eyles

ABSTRACT

Laguna Potrok Aike, located in southernmost Patagonia (Argentina, 52°S) is a 100 m deep hydrologically closed lake that probably provides the only continental southern Patagonian archive covering a long and continuous interval of several glacial to interglacial cycles. In the context of the planned 'International Continental Scientific Drilling Program' initiative 'Potrok Aike Maar Lake Sediment Archive Drilling Project', several seismic site surveys that characterize in detail the sedimentary subsurface of the lake have been undertaken. Long sediment cores recovered the material to date and calibrate these seismic data. Laguna Potrok Aike is rimmed steeply, circular in shape with a diameter of ~3·5 km and is surrounded by a series of subaerial palaeoshorelines, reflecting varying lake-level highstands and lowstands. Seismic data indicate a basinwide erosional unconformity that occurs consistently on the shoulder of the lake down to a depth of −33 m (below 2003 AD lake level), marking the lowest lake level during Late Glacial to Holocene times. Cores that penetrate this unconformity comprise Marine Isotope Stage 3-dated sediments (45 kyr BP) ~3·5 m below, and post-6800 cal yr BP transgressional sediments above the unconformity. This Middle Holocene transgression following an unprecedented lake-level lowstand marks the onset of a stepwise change in moisture, as shown by a series of up to 11 buried palaeoshorelines that were formed during lake-level stillstands at depths between −30 and −12 m. Two series of regressive shorelines between ~5800 to 5400 and ~4700 to 4000 cal yr BP interrupt the overall transgressional trend. In the basin, mound-like drift sediments occur after ~6000 cal yr BP, documenting the onset of lake currents triggered by a latitudinal shift or an increase in wind intensity of the Southern Hemispheric Westerlies over Laguna Potrok Aike at that time. Furthermore, several well-defined lateral slides can be recognized. The majority of these slides occurred during the mid-Holocene lake-level lowering when the slopes became rapidly sediment-charged because of erosion from the exposed shoulder sediments. Around 7800 and 4900 cal yr BP, several slides went down simultaneously, probably triggered by seismic shaking.

Keywords Lake-level changes, lake sediments, maar lake, palaeoclimate, Patagonia, seismic stratigraphy, Westerlies.

INTRODUCTION

With maximum latitude reaching more than 55°S, Patagonia in southernmost South America is the only large landmass located close to Antarctica (Fig. 1). Its continental climate archives thus play an important role in deciphering the timing and amplitudes of past climate change in the southern hemisphere. These records are crucial for investigating the synchronicity of globally observed abrupt events, a key also to establishing and validating global climate models (Ariztegui *et al.*,1997; Bard *et al.*, 1997; Markgraf *et al.*, 2000). Geological climate archives from Patagonia consequently provide crucial elements that are able to link records from Antarctica with the currently better-studied archives from the tropics and the northern hemisphere.

The climate of Patagonia is influenced highly by the Southern Hemisphere Westerlies wind system that controls moisture distribution at these high latitudes. Several studies have shown variations of the Southern Westerlies through the Late Glacial and the Holocene (Markgraf, 1993; Lamy *et al.*, 2001; Gilli *et al.*, 2005b; Mayr *et al.*, 2007). The hydrological balance of Patagonia and the associated wind regime furthermore are connected to the occurrence of polar outbreaks of Antarctic cool air masses (Marengo & Rogers, 2001) and to oceanographic processes such as the upwelling of cool Antarctic deep water and the Antarctic Circum Polar Flow (Lamy *et al.*, 2002). In addition to studies of Patagonian peat bogs (e.g. Markgraf, 1993; Heusser, 1995) and Andean ice cores (Thompson *et al.*, 2000), lake sediments from southern Patagonia provide high-quality sensitive and continuous records to reconstruct past fluctuations of this climate system, as long as the 'right' lakes and the ideal coring locations are chosen (Ariztegui *et al.*, 2000; Ariztegui *et al.*, in press). Examples include the hydrologically closed extra-Andean lake basin of Lago Cardiel (Fig. 1) located at 49°S (Gilli *et al.*, 2001, 2005a,b; Markgraf *et al.*, 2003) that contains a record spanning over 20 kyr, or glacial lakes from the Andean realm (Ariztegui *et al.*, 1997), covering a Late Glacial to Holocene time span. While several studies of lake sediments exist north of 50°S, only a few lakes have been investigated further south (Waldmann *et al.*, 2008). Here, a study of Laguna Potrok Aike at 52°S is presented, that is potentially the only lake in southern South America holding a record that spans several glacial to interglacial cycles (Zolitschka *et al.*, 2006).

In addition to providing palaeoclimate data, the present study also investigates how the sedimentary architecture in closed lake basins responds to changes in the hydrological budget (i.e. lake-level fluctuations and shoreline development: Seltzer *et al.*, 1998; Balch *et al.*, 2005; Brooks *et al.*, 2005;

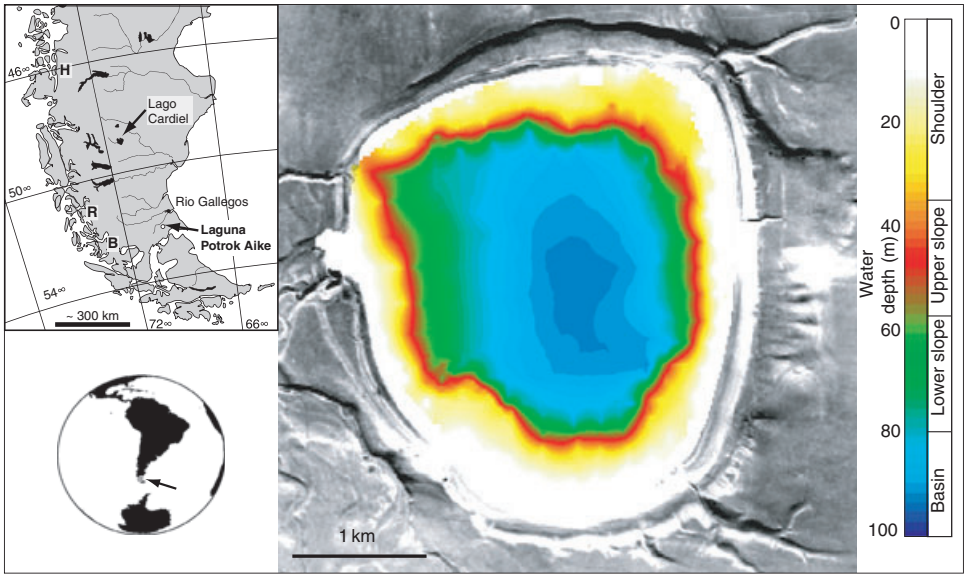

Fig. 1. Aerial photography of Laguna Potrok Aike together with bathymetry based on seismic surveys. Inserts show location of the lake in southern South America. The volcanoes Reclús (R), Hudson (H) and Mt. Burney (B) are marked with capital letters. Note the elevated beach ridges and river cut-throughs marking former lake-level highstands. Bathymetric data obtained and interpolated from 3·5 kHz seismic data converted to depth with a V_p = 1460 m sec^{-1}.

Gilli *et al.*, 2001, 2005b). The large suite of geophysical data collected in Laguna Potrok Aike helps to link the subsurface of the lake and the modern lake-floor morphology with the subaerially exposed deposits from previous lake-level highstands. The resulting past lake-level evolution is thus not only a relative record of wetter and dryer periods, but also provides quantitative information because it is based on a dated subaquatic and subaerial succession of shorelines.

STUDY AREA

Laguna Potrok Aike, located at 52°S, 70°W at an elevation of 113 m above sea-level in the steppe region of Patagonia (Fig. 1), is a 100 m deep and 3·5 km wide almost-circular crater lake that was created by an explosive eruption caused by the contact of rising magma with groundwater. Its formation is Ar/Ar-dated from the phreatomagmatic tephra on glass fragments as 0·77 ± 0·24 Ma (Zolitschka *et al.*, 2006). Annual precipitation amounts to <200 mm and the mean annual temperature is 7·4 °C (Zolitschka *et al.*, 2006). The lake lies in the regime of the Southern Westerlies, characterized by: (i) high wind speeds with mean annual values of 7·4 m sec^{-1} and mean monthly values in early summer of 9 m sec^{-1}; and (ii) wind directions primarily from the west shifting occasionally to NW and SW (Endlicher, 1993; Baruth *et al.*, 1998). Depending on the wind pattern, the lake lies in the influence of the tephra plumes from eruptions of Andean volcanoes such as Hudson, Reclús and Mt. Burney (Fig. 1). The lake is hydrologically closed, so that its water level is highly sensitive to changes in the precipitation/evaporation ratio (P/E). This dependence has been shown through a modelling study of the hydrological balance incorporating instrumental meteorological and stable isotope data and bathymetric information which was validated for the period 2001 to 2005 AD. The high depth-to-area ratio of the lake underlines its potential to hold a continuous sedimentary record that was unaffected by desiccation processes and was furthermore spared from Late Quaternary glaciations.

The modern limnological regime in the lake is influenced by one major inflow that is active today only after major rainfall when it supplies suspended sediment from the catchment area. These particles are mixed with aeolian particles that may reach significant amounts because of high maximum wind speeds. Physical water column data show that there is almost no stratification of the water body under present-day conditions. This effect is due to the strong winds that enforce polymictic conditions and hardly allow the formation of a thermally stratified water body during southern summers. The winds, and resulting up to 1·5 m high waves, furthermore trigger longshore currents that transport gravel and sand, forming characteristic gravel ridges in the surf zone of the beaches.

As part of the same initiative aimed at generating scientific and financial leverage for a deep drilling campaign (Zolitschka *et al.*, 2006), the sediments of the lake were recovered with numerous short cores (Haberzettl *et al.*, 2005, 2006) and with two long cores that were investigated for sedimentological and geochemical proxies (Haberzettl *et al.*, 2007, 2008), as well as for the pollen record (Mayr *et al.*, 2007; Wille *et al.*, 2007). The seismic–stratigraphic results and their palaeoenvironmental implications obtained by the analysis of a series of seismic data sets that were calibrated chronostratigraphically and sedimentologically by using the same set of long cores are presented here. This study shows how the dated changes in sedimentary architecture can be applied towards a quantitative reconstruction of past environmental change, taking full advantage of a lake system in which lake level varies as a function of the past hydrological balance.

METHODS

In February and March 2003, the subsurface of Laguna Potrok Aike was investigated with a high-resolution 3·5 kHz seismic system deployed from the steel-hulled catamaran *RV Lago Cardiel*, which was used for all other consecutive seismic surveys as well. The pinger instrument allows a penetration of several tens of metres with a vertical resolution of less than 10 cm. The signal was recorded digitally in the SEG-Y format. The shot interval was 500 msec and cruising speed approximately 6 km h^{-1}. Positioning data were obtained by a GPS system mounted directly on the sender/receiver assembly. Over 100 km of seismic lines were acquired, imaging the subsurface of the lake with a dense grid of 10 east–west lines, eight north–south lines and some additional lines in selected areas (Fig. 2). Average line spacing amounts to 250 m. Single-channel data were processed by applying a bandpass filter (2 to

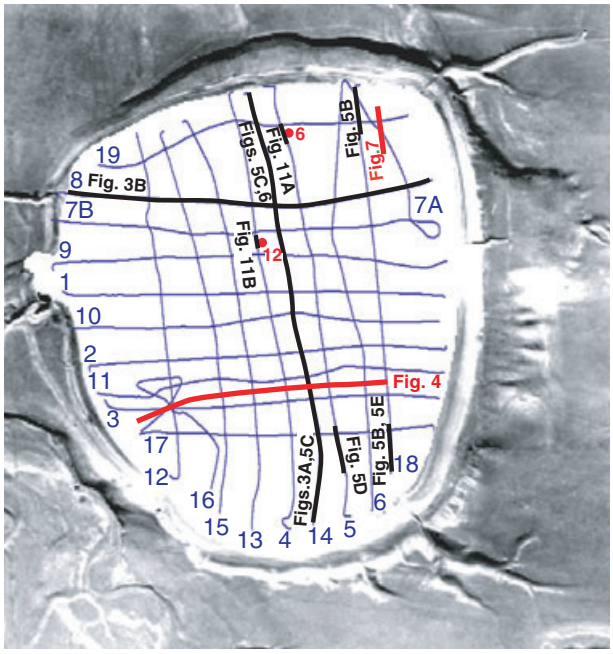

Fig. 2. Map with grid and line numbers of the high-resolution 3·5 kHz pinger survey. Location of displayed pinger lines are indicated with bold black lines. Red lines mark sparker line shown in Fig. 7 and single-channel airgun line shown in Fig. 4. Locations of long piston cores are indicated with red dots (PTA03/06, PTA03/12).

6·5 kHz) and a broad automatic gain control (AGC; 200 msec window length). All seismic elevations refer to lake level during this survey (February/March 2003).

The second seismic campaign at Laguna Potrok Aike, in February 2004, was performed with two 1 $in.^3$ airguns as sources that were fired simultaneously every 4 sec, producing an acoustic signal with a central frequency of 200 to 300 Hz at a firing pressure of 70 to 80 MPa. The reflected signal was recorded with a 20-element single-channel streamer (4 m active length) with a built-in preamplifier. Thus, 13 seismic sections were acquired, three in the north–south direction and 10 in the east–west direction, all of which are 2 to 3 km in length. The data were recorded digitally in the SEG-Y format. Navigation data were obtained with conventional GPS written directly in the SEG-Y trace headers. The boat speed during acquisition was held constant at ~5·5 km h^{-1}, resulting in an average shot spacing of 6 m. Processing of the single-channel data consisted of a bandpass filtering (150/200 to 800/1000 Hz), a constant gain (no AGC), a water-bottom muting and a trace mixing (1-3-1) that increased the lateral coherence of the primary reflections, thus improving the signal-to-noise ratio.

The third seismic campaign at Laguna Potrok Aike was performed in December 2004 with a sparker source and a single-channel streamer, which were both towed at the water surface. During four days of data acquisition, a regional seismic grid across the entire lake, two additional denser grids in areas of special interest and some 'horizontal stacking profiles' were acquired. In total, 74 high-resolution sparker profiles (~110 km total length) were recorded. The sparker source was operated at 300 J and produced an acoustic signal of 150 to 1500 Hz. A single-channel high-resolution streamer was used for the detection of the seismic reflections. This streamer has an active length of 2·7 m and consists of 10 hydrophones with 0·3 m spacing. The detected signal is preamplified in the streamer. A 200 to 2300 Hz bandpass filter was applied. The filtered signal was recorded digitally and converted to the SEG-Y format. Positioning data were obtained by GPS and recorded directly in the seismic headers. Post-processing includes further filtering, AGC and spiking and/or predictive deconvolution.

In order to obtain a better insight into the general maar geometry and the deeper sedimentary layers, an additional seismic pre-site survey was carried out in spring 2005 with a 40 $in.^3$ Mini-G airgun as the acoustic source.

Using a manual percussion piston coring system, a 9 m long core (PTA03/06) was retrieved from the lake shoulder in austral summer 2003 in a water depth of ~30 m (Haberzettl *et al.*, 2008). With the same equipment, two overlapping cores (PTA03/12 + 13) were recovered from the 100 m deep central basin (Haberzettl *et al.*, 2007). Cores were scanned with a Multisensor Core Logger (MSCL) yielding the bulk-density curves used for the seismic-to-core correlation. Composite sections at both sites were defined using visual core overlaps and matching calcium profiles obtained by X-ray fluorescence (XRF) scanning.

Radiocarbon ages were obtained on both cores from aquatic and terrestrial macroremains, inorganic carbonate samples and bones (Haberzettl *et al.*, 2007, 2008). Previous studies have shown that Laguna Potrok Aike sediments do not contain amounts of old carbon so that hard-water effects can be discarded (Haberzettl *et al.*, 2005). Data were calibrated using Reimer *et al.* (2004) and the software CALIB 5·02 (Stuiver & Reimer, 1993; Stuiver *et al.*, 2005).

GEOMORPHOLOGY

The area surrounding the lake is characterized by a series of palaeoshorelines, as high as 21 m above modern lake level, which are often cross-cut by fluvial incisions (Fig. 1). Most of these currently dry incisions descend all the way to the modern lake shore, but all of them are much wider and deeper above than below the highest exposed palaeoshorelines, where they form only narrow and barely visible valleys (see NE and SE corner of Fig. 1). This geomorphological pattern clearly witnesses lake stages during the past, when the lake level was higher and the rivers were carrying significantly more water into a larger lake creating wider incisions.

The morphobathymetry of the almost circular-shaped lake is characterized by three morphological elements (Fig. 1):

1 A broad and gently dipping shoulder down to a maximum water depth of ~30 to 35 m that surrounds the entire lake. Only in the north-western corner is no such shoulder developed and the slope break is relatively close to the shore (Fig. 3B).

2 Steep slopes with angles up to 20° which descend from ~35 m down to a water depth of 70 to 90 m. These slopes are sometimes dissected by downslope incisions forming canyon-like structures (Fig. 3B).

3 The deep, rather flat basin in the central area of the lake that forms a slightly upward-concave bowl, with a maximum water depth of almost 100 m. Laterally, this deep central basin is cut abruptly by the surrounding steep sides. Only towards the western shore does the basin floor gradually rise from its maximum depth up to a water depth of ~70 m, before the steep rim cuts off this gently east-dipping basin floor (Figs 1 and 3B).

SEISMIC FACIES AND SEISMIC STRATIGRAPHY OF THE LACUSTRINE BASIN FILL

On the deep airgun data, more than 200 to 300 m of lacustrine sediments were imaged and combined in Seismic Unit I; they contrast with the other units, which comprise the surrounding and underlying partly brecciated volcanics (Seismic Unit II) and the bedrock (Seismic Unit III). The present study focuses solely on the upper part of these lacustrine sediments, Subunits I-a and I-b, to a maximum sub-lake-floor depth of ~40 m (Figs 3 and 4), whereas the deeper lacustrine infill and the morphology and structure of the bedrock and diatreme will be presented in a forthcoming publication.

Subunits I-a and I-b, which are defined on the lake shoulders where they are separated by a distinct unconformity, are merged into a composite Subunit I-ab in the deep basin, because they are not separated by any unconformity here and because the steep slopes do not permit tracing of the unconformity from the lake shoulders to the correlative conformity on the basin floor. A detailed seismic stratigraphy was performed by establishing seismic facies analyses, and by mapping unconformities and correlated conformities (Vail *et al.*, 1977), distinguishing areas with different seismic reflection characteristics as well as defining different seismic units (Figs 3 to 7).

The sedimentary subsurface of the three morphobathymetric units (shoulder, slope and basin) cannot be connected physically because of the steep slopes (Fig. 3). Because of the steep angle, these slopes are characterized by a low sedimentation rate and hence contain very little sediment. Only in some areas of the lower slope, especially in the south-western and north-eastern areas of the basin, where the slope angles are slightly lower, can up to 40 m thick packages of sediment be discerned by subparallel steeply dipping reflections (Fig. 3B). The abrupt edges of these areas, however, do not allow for a physical connection to the basin and/or shoulder. As a consequence, the seismic stratigraphy is presented in two sections, one for the lake shoulder and the other for the basinal parts.

Lake shoulder

The subsurface reflections below the lake shoulder are characterized in the 3·5 kHz data by a highly reflective seismic pattern with maximum penetration of around 20 m (Fig. 5). Subunits I-a and I-b can only be discerned here, where they are separated by a major unconformity. The upper ~5 to 10 m that defines Subunit I-a consists of draping, slightly basinward-dipping reflections that terminate laterally when the slope becomes steeper. This subunit conformably overlies an erosional unconformity (e), marked as a blue horizon on all sections (Figs 3 and 5). The erosional unconformity occurs persistently around the entire lake, truncating reflections of the underlying upper slope section (Fig. 5A). The

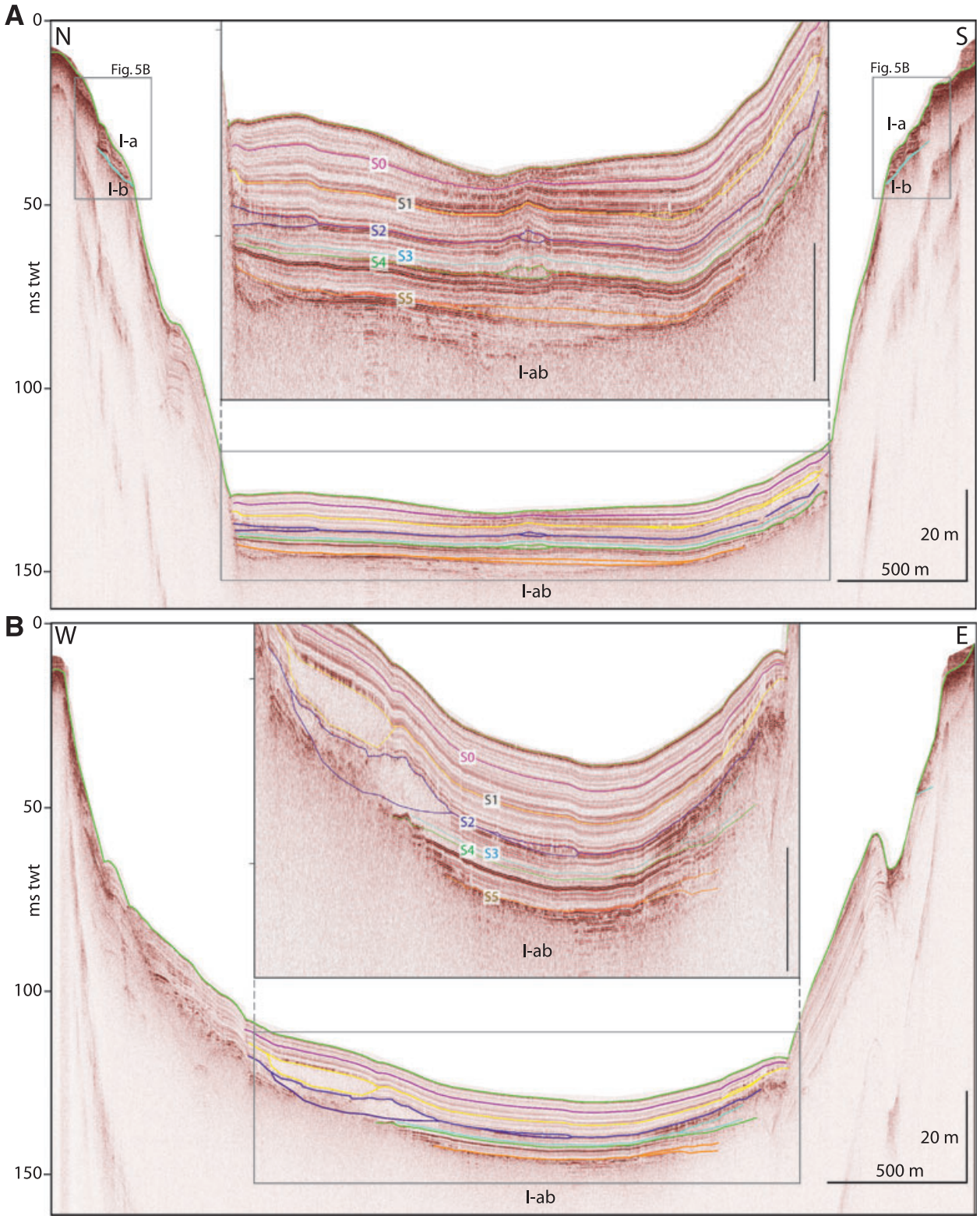

Fig. 3. Two 3·5 kHz seismic sections crossing the entire lake (note vertical exaggeration). The unmuted sections in the marginal areas at shallow depths image the seismic energy reflected by dense aquatic vegetation. (A) Line 14 from north to south. (B) Line 8 from west to east. Rectangles mark detailed views shown in inserts and in Fig. 5B. Event horizons in the basinal area (lines with various colours) and unconformity on the lake shoulders (blue line) are indicated. The seismic-stratigraphic basinal event horizons S0 to S5 are defined by the occurrence of seismically transparent mass-flow units (lateral slides). Note in both examples the simultaneous occurrence of two mass-flow units at event horizon S2 and the 'canyon'-like incision on the eastern shore (B).

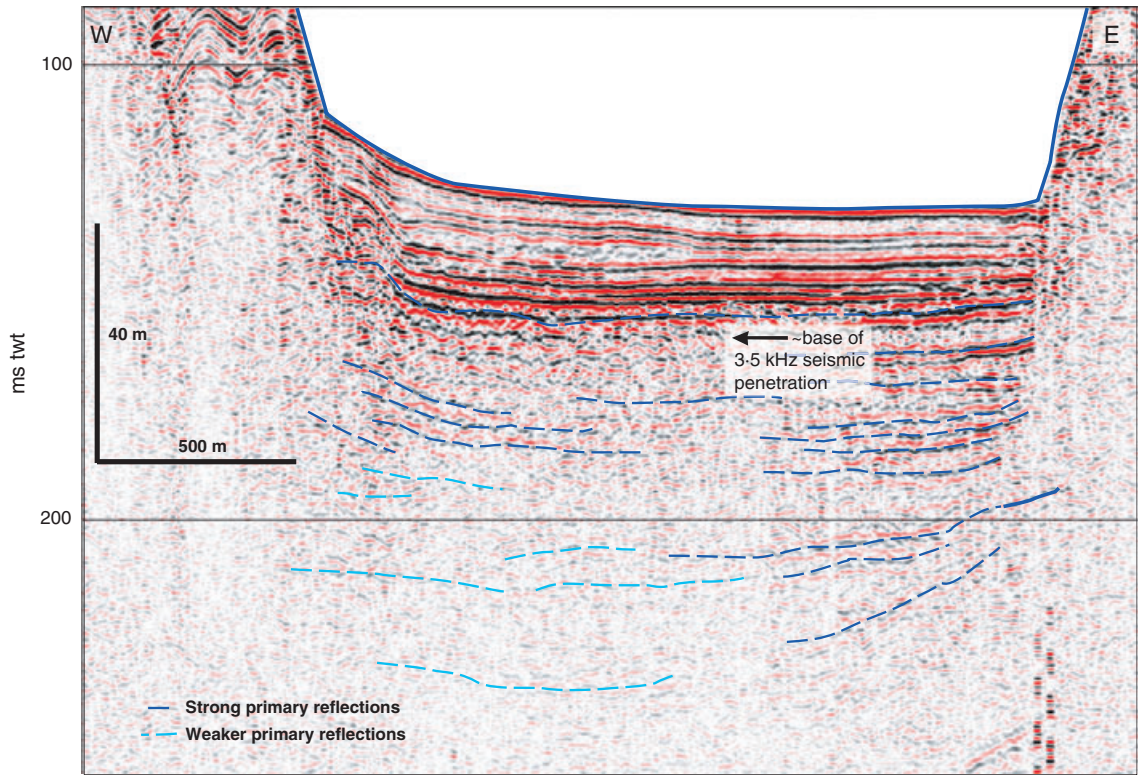

Fig. 4. Single-channel airgun line 8 that shows some deeper reflections (interpreted with dashed blue lines) indicating the bowl-shaped 'layer-cake' stratigraphy.

unconformity itself also dips gently basinward (Fig. 8), almost crops out and merges below 45 msec two-way-travel-time (twt) or 33 m water depth into its correlative conformity that barely is trackable on the seismic data and follows the steep slopes in the shallow subsurface (Fig. 5). Several internally transparent, lens-shaped, convex-upward sediment bodies occur on top of that unconformity or on horizons within Subunit I-a (numbered 1 to 11 in Figs 5 and 6; Table 1). These units are capped by high-amplitude reflections and do not allow further penetration of the acoustic signal so that they mask the underlying succession. These features always have flat landward parts and steeper fronts facing the lake and reach widths of 50 m and heights of less than 5 m; they occur all around the lake at consistent water depths. However, these features are more frequent along the northern and southern margin than along the western and eastern lake shoulder. The deepest one (1) always directly overlies the unconformity (Fig. 5B), whereas the shallower ones occur at stratigraphically higher levels. While the northern margin usually displays an incomplete succession of these features at continuously decreasing water depths and increasingly higher stratigraphic levels (Fig. 5), the southern margin (in particular, the south-eastern area of the lake, Fig. 5C and D) is characterized by a more complete and also more complex sedimentary architecture. Up to 11 features are recognized here (1 to 11) which form a stratigraphic succession in alternating increasing and decreasing water depths. These features can be tracked on the shoulder from their thin lakeward equivalents to the mound-like marginal buildups. The general morphobathymetric bulge on the shoulder surrounding the entire lake between 20 and 30 msec twt is formed mainly by the complex lateral and vertical stacking of these transparent mounds. Along the northern shoulder, where core data are available, three seismic horizons were tracked within Subunit I-a in order to establish a seismic-to-core correlation. These three horizons a, b and c are the lakeward equivalent of the mound features 2, 4 and 9, respectively (Fig. 6).

Below the unconformity, the truncated Subunit I-b displays a thick package of steeply (up to 10°) lakeward-dipping, intermediate-amplitude reflections that merge into the steep slope (Figs 5A and 7); they mostly overlie the top of the similarly dipping acoustic basement defined on sparker and pinger data.

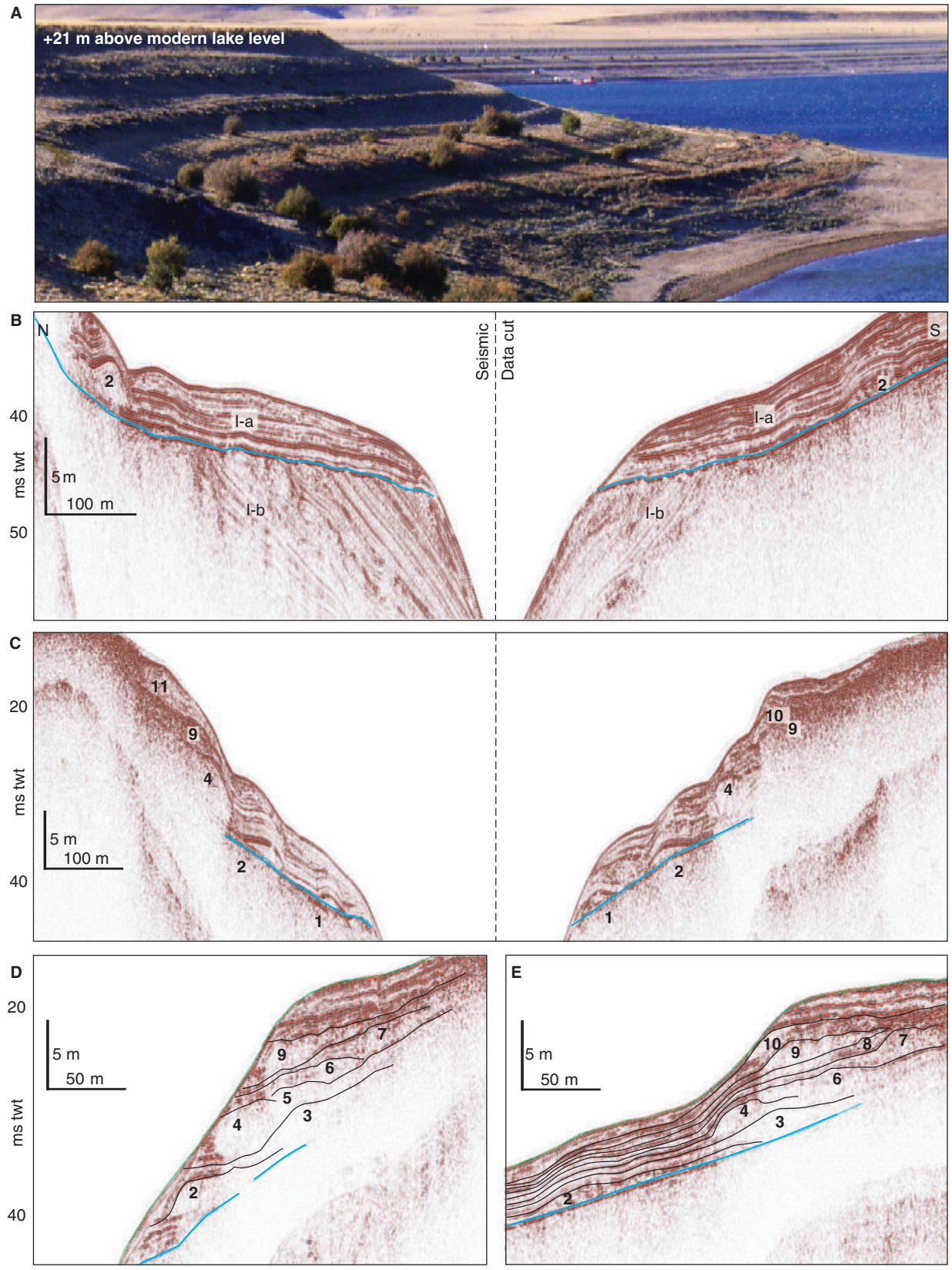

Fig. 5. (A) View of succession of subaerially exposed palaeoshorelines surrounding Laguna Potrok Aike, witnessing lake-level highstands. (B) to (E) 3·5 kHz seismic lines showing lake shoulders in the lake marginal areas (vertical exaggeration 10 to 20 times). Blue line marks erosional unconformity separating seismic sequences I-a and I-b. Bold numbers refer to submerged palaeoshorelines in stratigraphic order (see Table 1). For location see Fig. 2. (B) Northern and southern segment of Line 18. Note angular unconformity caused by subaerial erosion of underlying upper slope sediments during maximal lake-level lowstand at 45 msec per 33 m. (C) Northern and southern end of Line 14. Note lens-shaped seismically transparent units that formed on unconformity during transgression with steep basinward and flat landward side marked by bold numbers; they are interpreted as beach ridges (palaeoshorelines) formed during lake-level stillstands. (D) Southern end of Line 5 and (E) southern end of Line 18 (continuation of B): The palaeoshorelines are stacked vertically and laterally and reveal a prograding and retrograding succession determined by lake-level changes.

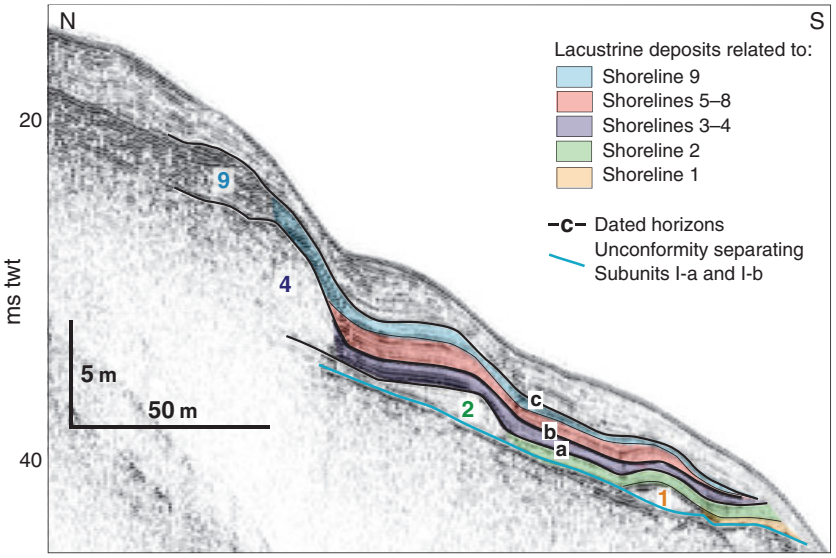

Fig. 6. Northern end of Line 14 (as Fig. 5C) with interpreted and numbered palaeoshorelines (Fig. 5; Table 1) and identified seismic-stratigraphic horizons (a to c). These lacustrine horizons can be linked seismically to palaeoshorelines (a = 2, b = 4, c = 9) allowing determination of palaeo-lake levels. All three horizons can be correlated through seismic lines 19 and 5 to the coring site of PTA03/06, enabling assignment of a chronostratigraphic age using the seismic-to-core correlation (Fig. 11) and the age model of the core.

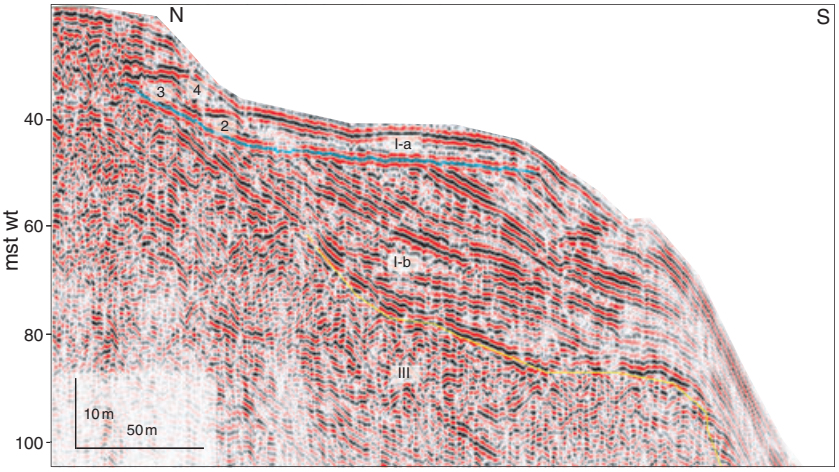

Fig. 7. Sparker seismic line 51 showing lacustrine Subunits I-a and I-b, separated by an erosional unconformity (blue line). Sediments of Subunit I-b display lakeward dip of up to 10° and overlay the similarly inclined bedrock surface (Seismic unit III below yellow line). Arabic numbers 2 to 4 indicate palaeoshoreline succession as shown in Figs 5 and 6.

In addition to sedimentary subsurface information, the 3·5 kHz seismic data are able to display a several metre-thick forest-like cover of subaquatic vegetation consisting of *Potamogeton* and *Myriophyllum* that grows on the lake floor down to a water depth of 15 to 20 m (Fig. 3A and B; reflections above green-marked lake floor on the margins).

Deep lake basin

Acoustic stacking velocities from multichannel data in the deep basin (Fig. 3) vary around 1550 m sec^{-1}, indicating unconsolidated lacustrine sediments. Seismic penetration of the 3·5 kHz signal into the central basin floor is

Table 1. Palaeoshorelines numbered in stratigraphic order with interpreted palaeowater-level in milliseconds two-way-time (msec twt) and metres below the 2003 lake level.

Palaeoshoreline in stratigraphic order	Approximate water depth (msec twt)	Approximate water depth (m, @1450 m sec^{-1})	Approx. age (cal yr BP)
11	16	12	
10	22	16	
9	24	17	~4300
8	23	17	
7	22	16	
6	25	18	
5	27	20	
4	30	22	~5400
3	29	21	
2	37	27	~6100
1	42	30	
Lowest erosion	45	33	> 6800

The approximate ages are obtained by seismic-stratigraphic correlation from core PTA03/06 (Haberzettl *et al.*, 2008).

limited to 15 to 20 m and only images Subunit I-ab (Fig. 3). In some small windows up to 40 m of sediment can be observed, especially in the south-eastern area of the deep basin. The energy of the 3·5 kHz signal usually fades below some last high-amplitude reflections that are stacked laterally and not tied to a particular seismic horizon (Fig. 3), a pattern indicative of higher gas content. Single-channel airgun data (Fig. 4) yield information down to a sub-lake-floor depth of over ~100 m until reflected energy fades. Layering is mostly subparallel to the overlying lake floor and no major unconformities can be seen in the basinal section, indicating that the sedimentary succession continues downward in a 'layer-cake' fashion. Within Subunit I-ab, two major seismic facies can be discerned: (i) laterally continuous reflections of high to medium amplitudes that display a draping pattern of sediment infill, locally intercalated by (ii) a number of seismically transparent lens-shaped units with well-defined outer boundaries (Fig. 3). The trans-

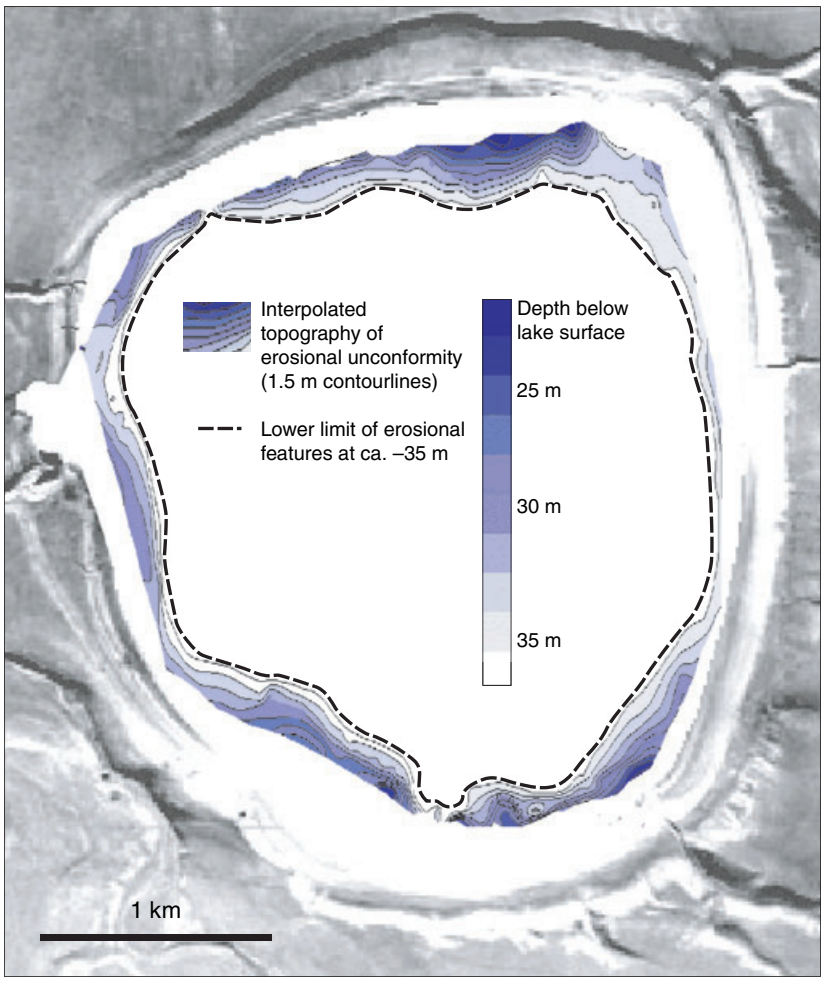

Fig. 8. Map showing palaeotopography of subaerial unconformity on the lake shoulders at the time of maximum lowstand. Bold-black dashed line indicates reduced area of lake during the −33 m lake-level lowering.

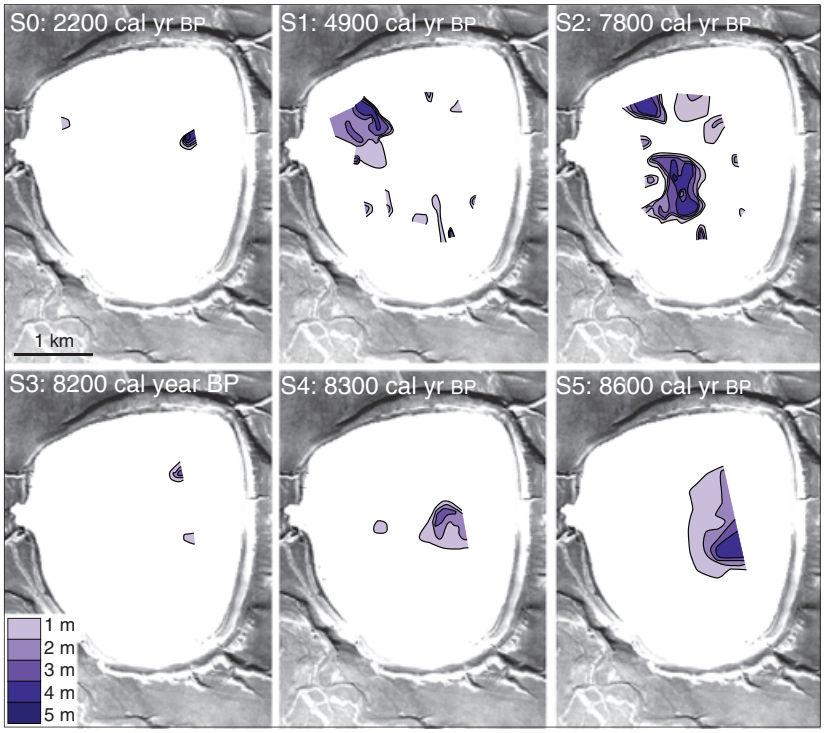

Fig. 9. Aerial distribution map of mass flows belonging to each of the S0 to S5 event horizons. S1 and S2 both display almost 10 individual flows that were triggered simultaneously. This effect is indicative of a common trigger mechanism, probably seismic shaking.

parent units often produce upward-concave morphologies and either wedge out basinward into hummocky-shaped tongues or transform laterally along sharp and steep facies boundaries into the seismically well-layered facies. The lateral extent of several hundreds of metres, the occurrence in variable water depths, the lack of capping high-amplitude reflections and the fact that the seismic signal is able to image the underlying section (Fig. 3) clearly distinguish these features from the mound-like features found on the lake shoulder (Fig. 5). Within the upper part of Subunit I-ab, these features occur at six stratigraphic levels which have been named and mapped throughout the basin (S0 to S5; Figs 3 and 9). The tops of these units represent the stratigraphic time at which these deposits were formed, whereas the bases of these units represent just a facies boundary and may cross-cut timelines (Fig. 3).

Although the overall sedimentation pattern of the basinal subsurface is rather of draping geometry, the units above the S1 horizon are characterized by long (up to ~1 km) elongated mounded geometries on the northern and southern basin edge, indicating areas of higher sedimentation rate (Fig. 3A), whereas the basin-central east–west axis is rather sediment-starved. This change in sediment distribution pattern, which starts gradually between the S2 and the S1 horizons, must be caused by a sediment-focusing mechanism. The related change is also shown on the interpolated sediment thickness maps of pre-S1 and post-S1 intervals (Fig. 10).

CALIBRATION WITH LONG PISTON CORES AND CHRONOSTRATIGRAPHY

Two dated long sediment cores, one from the lake shoulder and one from the central basin floor, are available to calibrate these seismic data from a sedimentological, petrophysical and chronostratigraphical perspective.

Lake shoulder

Core PTA03/06 (9 m long) has been taken on the northern lake shoulder at a water depth of ~30 m (Figs 2 and 11A; Haberzettl *et al.*, 2008). Two major lithological units can be distinguished: the upper unit from 0 to 311 cm consists of dark brown to black silts with abundant gastropods. Towards the base of this unit, plant debris occurs frequently. The entire unit is characterized by very low wet-bulk-density values around 1·2 g cm^{-3} and coincides with seismic Subunit I-a (V_p = 1500 m sec^{-1} for this unit). It is separated from the underlying lithological unit by a greenish-brown fine-sandy layer, which represents a reworked layer with abundant

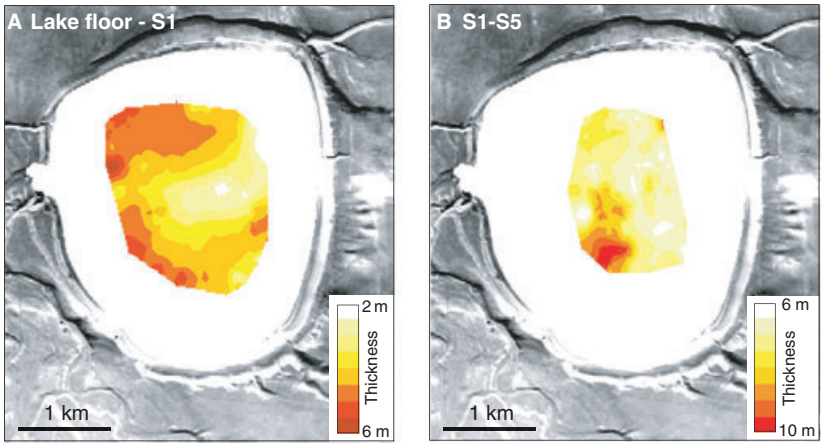

Fig. 10. Map of sediment thickness in the basinal area for two periods (note different scales for thickness). (A) Sediment thickness between the modern lake floor and the S1 event horizon (0 to 4860 cal yr BP). Note the reduced sediment thickness in the central part and the dome-shaped depocentres, caused by lake currents redistributing sediments to areas of low current velocity. (B) Sediment thickness between the S1 and the S5 event horizons (4860 to 8630 cal yr BP). Sediment thickness wedges towards the western shore indicating accumulation by underflows originating from the major inflows and mass flows at the toe-of-slope. The basinal section shows a rather draping pattern without major contrasts in sediment thickness, indicating no occurrence of lake currents.

macroremains (Haberzettl *et al.*, 2008), and which is marked by a distinct downward increase in bulk density to values around 2 g cm^{-3} (V_p of 1600 m sec^{-1} for core-seismic correlation of seismic Subunit I-b) (Fig. 11A). This boundary coincides with the high-amplitude erosional unconformity (e) and represents the boundary between seismic Subunits I-a and I-b (Fig. 11A). The remainder of the core (379 to 900 cm) consists of greenish-brown fine sand with few silt and tephra layers and very few macro-remains. One radiocarbon age has been determined below the unconformity, providing a Marine Isotope Stage (MIS) 3 age for this unit (44·8 ^{14}C kyr BP at 7·3 m). The reworked layer above was deposited after ~6800 cal yr BP. Two more dates in the upper unit define a Late Holocene age model (Haberzettl *et al.*, 2008) and yield ages of 6100, 5400 and 4300 cal yr BP for seismic horizons a, b and c, respectively (Figs 6 and 11A, Table 1).

Deep lake basin

Composite core PTA03/12 + 13 (19 m long) was recovered just north of the centre of the deep basin at a water depth of ~100 m (Figs 2 and 11B; Haberzettl *et al.*, 2007). In general, the core consists of clayey and sandy silts that become coarser with depth. The top 6 m is laminated and, below 3 m, is rich in gastropods. From 6 to 13 m, the core consists mostly of dark grey homogeneous medium to coarse silt very rich in gastropods. Two tephra layers occur in the lower part of this section (one from Hudson and one from Mt. Burney volcano; Haberzettl *et al.*, 2007, 2008). Another layer consisting of reworked Mt. Burney material was deposited a few centimetres above the original tephra. These three layers are characterized by prominent density peaks, resulting in an excellent match with three high-amplitude reflections on the seismic data (Fig. 11B; V_p = 1600 m sec^{-1}). Further downcore, gastropod content decreases and the core again becomes partly laminated. The bottom of the core consists of a Reclús Volcano tephra (partly reworked) underlain by a layer rich in macro-remains. The age–depth model is based on 16 radiocarbon ages as well as on the Mt. Burney tephra (Haberzettl *et al.*, 2007). The age at the base of the core was determined to be ~16 000 cal yr BP and no hiatuses occur in this basinal section. The resulting sedimentation rate shows a remarkable period, with an increased sedimentation rate between 8700 and 7300 cal yr BP (Fig. 12).

SEISMIC-STRATIGRAPHIC AND DEPOSITIONAL INTERPRETATIONS: IMPLICATIONS FOR PALAEOENVIRONMENTAL HISTORY

Subunits I-a and I-b on shoulder

The consistent water depth of 33 m, marking the deepest observed erosion of the unconformity 'e'

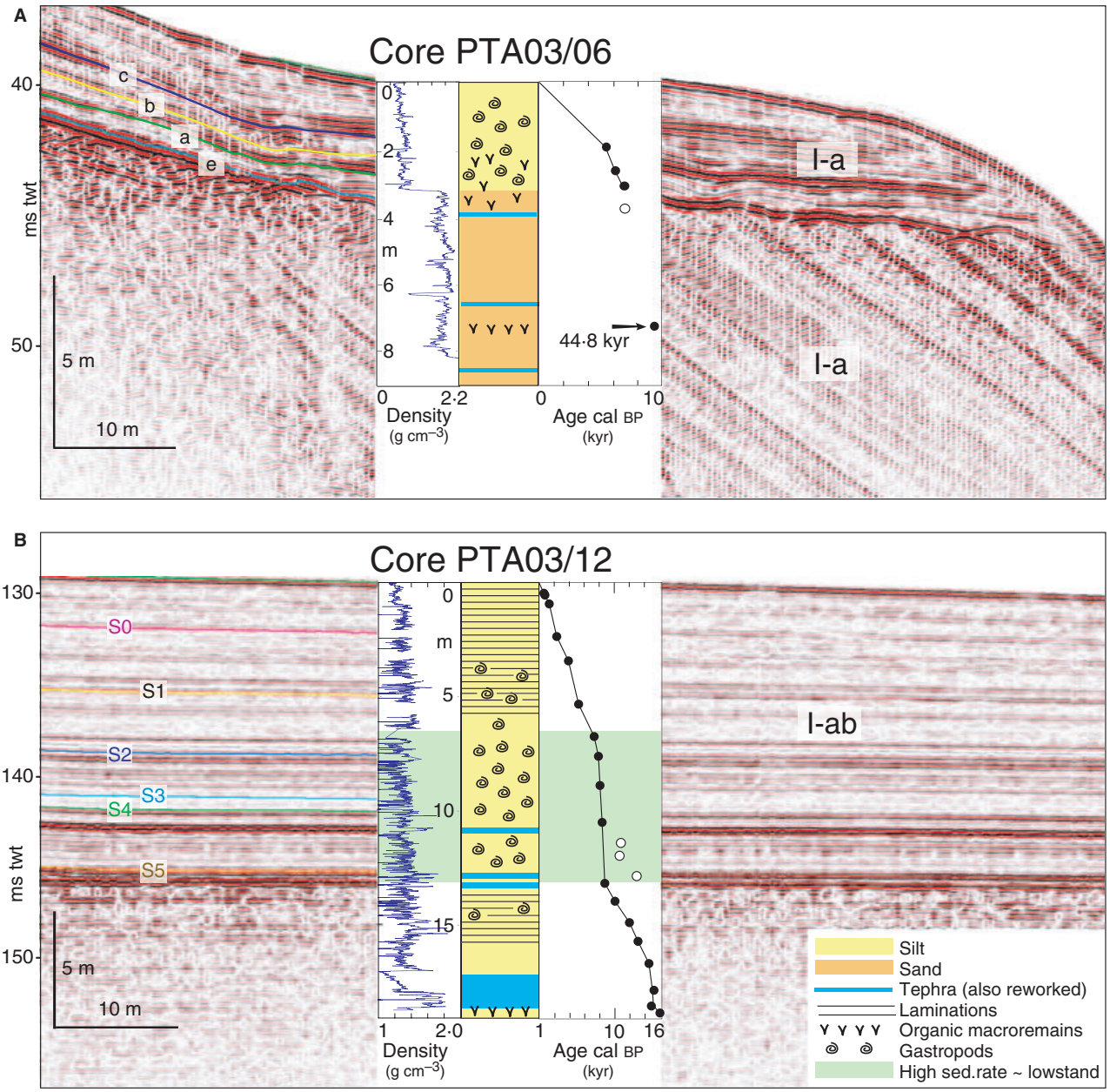

Fig. 11. Petrophysical properties (MSCL bulk density) with age-depth models based on AMS ^{14}C data of long piston cores and lithological column (Haberzettl *et al.*, 2007, 2008) superimposed on seismic sections at coring sites. For locations see Fig. 2. Open circles in age–depth graph indicate values not used for age model (roots and bioturbation in A; reworked material in B). (A) Core PTA03/06 from the shoulder area superimposed on Line 5. Note the sharp downcore increase in density at ~3 m coinciding with a major hiatus and unconformity separating low-density silty sediments above (younger than 6800 cal yr BP) from coarser high-density sandy sediments below (dated 44800 kyr BP at a depth of 7·3 m). For time-to-depth conversion, an average velocity of 1500 m sec^{-1} was used for the upper part, and 1600 m sec^{-1} for the lower part. (B) Core PTA03/12 from the basinal part superimposed on Line 4. Note the good match between the three high-amplitude reflections from ~11 to 13 m and the occurrence of tephra layers characterized by high-density values causing the prominent reflections. For time-to-depth conversion, an average velocity of 1600 m sec^{-1} was used for the entire section.

all around the lake, points clearly towards a significant lake-level lowering of ~33 m and rules out any local effects such as sediment removal through sliding or slumping. During this low-stand phase, subaerial exposure led to the erosion of upper-slope sediments that had been deposited during previous lake-level highstands (Figs 5A and 12). Because no deeper erosion can be

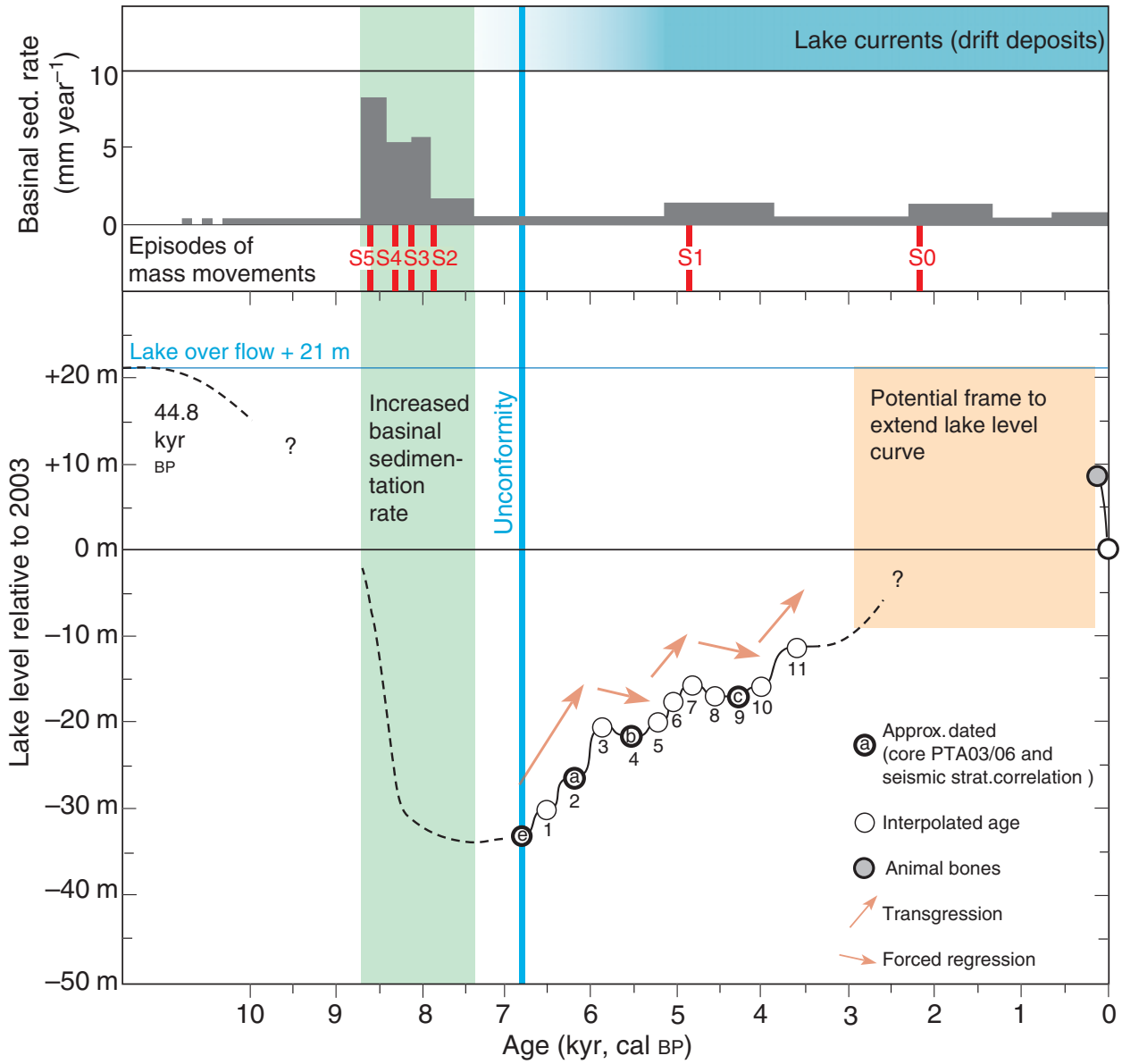

Fig. 12. Comparison of onset of drift deposition (lake currents), basinal sedimentation rates (Haberzettl *et al.*, 2007), occurrence of lateral mass-flow events (above) and lake-level fluctuations based on palaeoshoreline reconstructions (below). Circles indicate palaeoshorelines elevations and dates. Numbers under circles refer to the chronological order of shorelines mapped on the seismic data. The left edge of the plot is on an expanded time scale to accommodate for the 44·8 kyr BP date. Note the dramatically increased sedimentation rate during a lake-level lowering that exposes and erodes lake sediments on the lake shoulders. This event charges slopes rapidly so that it coincides with a series of lateral mass flows.

observed, it is certain that lake level did not fall beyond this depth and that Laguna Potrok Aike never fell dry, at least during the more recent history of more than 45 kyr (minimal age of Subunit I-b sediments). During the time of low lake level, the exposed sediments that today underlie the unconformity formed a gently dipping lake shore, with erosion being deepest close to, or even just below, lake level, where wave action is most efficient. This effect is shown by the interpolated morphology of the unconformity that shows the extent of the palaeolake and the topography of the exposed bowl-shaped (always lakeward-dipping) coastal area (Fig. 8).

After this period of low lake level, a transgression was initiated that flooded the shore along the unconformity so that the erosional surface became conformably overlain by sediments of the younger Subunit I-a. The lens-shaped seismically transparent units within Subunit I-a that were

formed on top of the unconformity and that occur around the lake at consistent depths are interpreted as palaeoshorelines, which formed during slowdowns or stillstands within the overall transgression. This interpretation is supported both by the consistent depths at which these features occur and by their morphologies which are similar to those of lacustrine shorelines in other closed lake basins (Thompson, 1992; Adams & Wesnousky, 1998; Ibbeken & Warnke, 2000; Komatsu *et al.*, 2001; Gilli *et al.*, 2005a; Anselmetti *et al.*, 2006). The characteristic shape of these features, with a steep lakeward-facing side and a gentle-to-flat landward portion is very typical of beach ridges marking palaeoshorelines that can develop only when water level remains stable for a certain period. Furthermore, an implication of the good preservation of these palaeoshorelines is that the lake-level rises in between phases of palaeoshoreline development must have happened rather quickly so that previously deposited shorelines were not eroded straight away (Gilli *et al.*, 2005a, and references therein). The complete succession of palaeoshorelines in the south-eastern part of the lake basin (Fig. 5C and D) allows a detailed reconstruction of lake-level fluctuations. These 11 units are stratigraphically stacked and mark a temporal succession of formation levels, to which palaeolake-level positions can be assigned. Such a succession is reminiscent of marine coastal sequences that are influenced by sea-level fluctuations (Posamentier & Allen, 1999; Rabineau *et al.*, 2006). Depending on the accommodation space, which is controlled by sedimentation rate and water-level fluctuations (ignoring in this case subsidence rate, because time span is short and Potrok Aike is a closed basin), the 11 palaeolake-level indicators define a curve characterized by higher-order transgressions and regressions. While the successions from the end of the unconformity 'e' to 3, from 4 to 7, and from 10 to 11 reflect increasing lake levels (transgressions), the transitions 3 to 4 and especially 7 to 10 represent slightly decreasing lake levels, during which the shoreline was forced to move out and down towards the basin centre (Figs 5C, D and 12), as described in the marine realm by the term 'forced regression' (Hunt & Tucker, 1992; Posamentier & Allen, 1999; Plint & Nummedal, 2000). The south-eastern area, where these shorelines are best developed, lies just in front of the largest fluvial incision surrounding the lake (Fig. 1), documenting that the shorelines in this area might also be delta deposits, which were fed from a fluvial point source and became remobilized through wind-driven longshore currents feeding the laterally occurring beach ridges.

This succession of palaeoshoreline migrations defining the lake-level curve following the lake-level lowstand can be dated using the seismic stratigraphy that was calibrated by the available shoulder core from the northern margin of the lake (Figs 6 and 11A). The three dated horizons a, b and c (see above) can be connected seismically to the shorelines 2, 4 and 9, respectively, which enables the reconstructed lake-level curve to be fixed at three temporal tie points (Fig. 12). The ages of the remaining palaeoshorelines were interpolated linearly between these fix points, and the youngest section was completed with a date from a shoreline occurring at +9 m above the 2003 level, where a horse and guanaco skeleton allowed an age assignment to the ~18th/19th Century (i.e. Little Ice Age, Fig. 12; Haberzettl *et al.*, 2005). Between the last shoreline (11) and the +9 m level, the lake-level curve currently is not constrained. However, the possibility of the lake level falling below ~−12 m (orange area in Fig. 12) can be excluded because no younger shoreline at or below this depth is observed, and the older shorelines are covered by a thick undisturbed package of shoreline-distal deposits lacking erosional features (Fig. 5C and D).

The resulting calibrated lake-level curve reflects the stepwise P/E changes during the Late Holocene. The transgressions between shorelines 4 to 7 and 10 to 11 were confirmed independently by geochemical proxies of the deep-water core that displayed moist periods around 4800 and from 3900 to 3700 cal yr BP, respectively (Haberzettl *et al.*, 2007). The two periods of forced shoreline regressions between ~5800 and 5400 and from ~4700 to 4000 cal yr BP point towards reduced P/E ratios at that time, documenting a fluctuating evolution of the hydrological balance during the Holocene.

Subunit I-b always appears as a thick 10° lakeward-dipping sediment pile that covers the bedrock substrate. These reflections occasionally show some disturbed layering possibly due to downslope mass movements. Core PTA03/06 indicates that Subunit I-b is dominated by coarser grain-size compared with Subunit I-a above (Fig. 11B). Because these tilted layers occur all around the lake, a delta origin due to a river inflow can be excluded. These sediment particles rather derive from enhanced fluvial or possibly aeolian input at times of higher lake levels (possibly at the + 21 m overflow level) and

became redistributed all around the lake shoulders.

Subunit I-ab in the basin

The regular basinal seismic facies represents well-layered sediments characterized by rather draping geometries. This effect indicates that the dominant associated depositional process is of a (hemi-)pelagic nature and that only little lateral gravitational sediment processes, such as turbidites, occur. This well-bedded facies, however, is interrupted by seismically transparent units which wedge out or show some basinward-continuing onlapping tongues. These units are clearly a product of gravitational downslope transports caused by mass flows (Fig. 3). Almost identical structures were identified in other lakes (Chapron *et al.*, 1999; Schnellmann *et al.*, 2002, 2005; Moernaut *et al.*, 2006; Strasser *et al.*, 2006) where they were interpreted as a product of gravitational downslope transports caused by mass flows, triggered partly by seismic shaking. A common characteristic of these structures is that their lower boundary often marks a zone of *in situ* sediment deformation caused by the overriding mass flow and, consequently, does not represent a time line (Schnellmann *et al.*, 2005). In contrast, the top of these lateral slides marks a seismic-stratigraphic level that defines the onset of regular sedimentation after such a mass-flow event and can be traced as an event horizon through the entire basin. Consequently, seismic stratigraphy allows determination of whether some of these mass flows occurred simultaneously, a criterion that has been used to single out seismic shaking as the trigger mechanism (Schnellmann *et al.*, 2002; Moernaut *et al.*, 2006; Strasser *et al.*, 2006). Undertaking this approach for the Laguna Potrok Aike mass-flow deposits shows that two of the event horizons (S1 and S2) are each characterized by at least nine individual mass flows that occurred at the same time (Fig. 9). Three of the other horizons (S0, S3 and S4) each show two mass-flow deposits, whereas S5 is only defined by a single mass-flow deposit (Fig. 9). Using the age model of the basinal core (Haberzettl *et al.*, 2007), these six mass-flow events were dated and were found to have occurred during the last ~9000 years (Table 2).

A comparison with the time series of sedimentation rate from the basinal core and the timing of these events shows a striking coincidence of high sedimentation rate with the occurrence of mass flows. The four older events (S5 to S2) all occur within a relatively short time window between 8700 and 7800 cal yr BP that is characterized by a high sedimentation rate and by the major lake-level lowering (Fig. 12). This relationship between sedimentation rate and lake level is probably caused by the increased sediment input from the exposed and eroded lake terraces (Haberzettl *et al.*, 2007). This increase in sediment rate is even more remarkable, considering that, during the lake-level lowering, runoff and thus catchment erosion are rather reduced. This leaves only the exposed and reworked lake terraces or potentially an increased aeolian input as major sediment sources during that period. Such increased sediment charging on the subaquatic slopes negatively influences slope stability, because vertical load of the tilted strata directly increases downslope forces (Hampton *et al.*, 1996; Locat & Lee, 2002; Strasser *et al.*, 2007). Furthermore, the combination of rapidly deposited fine-grained sediments, potentially closing off pore water under undrained conditions, together with less overburden hydrostatic pressure because of a lower lake level, results in reduced effective pressure. As a result, pore-fluid overpressure may occur and further destabilize the charged slopes (Sultan *et al.*, 2004), explaining the correlation of mass-flow occurrence and increased sedimentation rate during a lake-level drop; this alone, however, cannot explain the fact

Table 2. Depth in msec two-way-travel time (twt), depth in metres below lake floor and age for horizons a to c and erosional unconformity e at coring site PTA03/06 (above) and for stratigraphic event horizons S0 to S5 at coring site PTA03/12 (below).

	Depth (twt below lake floor, msec)	Depth (m)	Age (cal yr BP)
Core PTA03/06			
c	2·0	1·5	4300
b	2·8	2·1	5400
a	3·5	2·6	6100
e	4·5	3·4	6800
Core PTA03/12			
S0	2·7	2·2	2200
S1	6·1	4·9	4900
S2	9·4	7·5	7800
S3	11·8	9·4	8200
S4	12·6	10·1	8300
S5	15·8	12·6	8600

Time-to-depth conversion is based on a velocity of 1600 m sec^{-1} (1500 m sec^{-1} above unconformity in core PTA03/06). Age models are based on Haberzettl *et al.* (2007, 2008).

that S2 and S1 are comprised of multiple mass flows. For these two cases, seismic shaking, as discussed above, is the most plausible trigger mechanism. The S1 event, in particular, occurring around 4900 cal yr BP under regular sedimentation conditions, was triggered probably by a palaeoearthquake. Previous studies have shown that basinwide sliding of lateral slopes usually requires a local intensity (European Macroseismic Scale) of ~7 (Monecke *et al.*, 2004). For S2, this intensity might be lower because it happened during the period of generally unfavourable slope-stability conditions, so that less seismic acceleration might have been required to trigger the large number of simultaneous slides.

The sediment mounds in the northern and southern areas of the basin floor, and the sediment-starved east–west axial through in the central basin (Figs 3A and 10), developed sometime between the S2 and the S1 horizon (i.e. ~6000 cal yr BP). Such a pattern requires a depositional mechanism that focuses sediments in depocentres while keeping other areas under a condensed sedimentation regime. Such mound-like features are attributed usually to drift or current-controlled deposits: slower currents cause increased deposition of suspended particles, whereas higher current velocities result in a higher transport potential and lower sedimentation rates. The basinal sediment core PTA03/12 + 13 is located just at the southern margin of the northern drift mound (Figs 2 and 10), where no anomaly in the sedimentation rates can be observed (Fig. 12). The observed pattern in Laguna Potrok Aike is highly reminiscent of sediment geometries found in Lago Cardiel (Patagonia 49°; Gilli *et al.*, 2001, 2005a,b; Markgraf *et al.*, 2003), where similar deposits have been interpreted to be the result of increasing wind stress because of a change in the strength of the Westerlies at that latitude. In a similar fashion, drift-influenced sediment geometries in Laguna Potrok Aike would require nucleation of strong currents which, considering the extreme wind regime of today at the Laguna Potrok Aike location with mean monthly wind speeds of 9 m sec^{-1} during early summer (Endlicher, 1993; Baruth *et al.*, 1998), would not be surprising. The fact that the lowest sedimentation rates occur in the centre of the lake could imply not only a single cell of a lake current but a wind-driven double convection cell with a central east-directed flow through the middle of the lake and marginal west-directed backflows, as observed also in other comparable lakes (Gilli *et al.*, 2005b and references therein). Alternatively, wind-induced surface stress could also create a vertical convection cell, as water moving to the east triggers a plunging current that causes the reduced sedimentation rate in the east–west central basinal axis (Fig. 10A) possibly linked with an upwelling at the western shore. In any case, current measurements would be required to prove such a lake circulation pattern. These sediment geometries, the interpreted onset of wind-driven lake currents and the related change in wind regime indicate a mid-Holocene strengthening of the Westerlies in the area after ~6000 cal yr BP. This observation matches the timing of wind strengthening postulated for Lago Cardiel 3° to the north (after 6800 cal yr BP), also on the basis of drift deposits (Gilli *et al.*, 2005b). However, the presented timing of wind strengthening is about 3000 years later than what was postulated on the basis of the Laguna Potrok Aike pollen record, which showed a change at 9200 cal yr BP (Mayr *et al.*, 2007). This discrepancy can be caused by a higher sensitivity of the pollen record to a more gentle increase of the Westerlies, while the more or less simultaneous triggering of lake currents for Laguna Potrok Aike and in Lago Cardiel might require a certain minimal threshold in wind speed that was reached only later in the wind history of southern Patagonia.

The deeper basinal sections appear to be similar in nature to the shallow subsurface (Fig. 4). The overall stratigraphic pattern of subparallel reflections with only the occasional occurrence of seismically transparent units representing local mass movements, together with the absence of major unconformities, point towards the high potential of these sediments to contain a continuous and undisturbed palaeoenvironmental archive which potentially dates back to the volcanic creation of this maar lake.

SUMMARY AND CONCLUSIONS

The presented seismic-stratigraphic study of the basin fill of Laguna Potrok Aike, calibrated with two long sediment cores, enables reconstruction of a series of palaeoenvironmental events that occurred during the Late Quaternary in Patagonia at 52°S. Quantified lake-level fluctuations of this closed basin reflect past changes in precipitation/evaporation ratio. Periods of enhanced sublacustrine mass movements are linked to changes in sedimentation rates and potentially to palaeoseismic triggers. Sediment

geometries reflect changes in lake currents that are controlled by fluctuations in the Southern Westerlies. All these events can be tracked in the seismic data and are summarized in the following event chronology:

1 A thick package of lake sediments can be imaged using seismic methods at the bottom of Laguna Potrok Aike, reflecting the potential of the lake as a palaeoenvironmental archive spanning several glacial–interglacial cycles. This extended and potentially continuous continental archive is unique for the entire Patagonia area.

2 Around 45 kyr BP, the lake level of Laguna Potrok Aike was high and sediments of seismic Subunit I-b were deposited on the upper slopes. The lateral continuity of these slope deposits suggests that the lake level was much higher than today and that the lake might have been at its overflow position of +21 m above the present-day level.

3 A major drop in the lake level occurred at ~8700 cal yr BP. Despite the decreasing runoff from the catchment, exposed and eroded lake terraces provided an efficient sediment source, explaining the increase in sediment supply to the basin floor during this period of lake-level lowstand.

4 Maximum lake-level lowering reached ~33 m below the lake level of today, as witnessed by a consistent erosional unconformity surrounding the entire lake. This lowest lake level is dated to ~6800 cal yr BP.

5 Four of six mass-wasting events originating from the lateral lake slopes coincided with this lake-level lowering and with the increased sedimentation rate between 8600 and 7800 cal yr BP. Slope stability during this period was reduced strongly, because the slopes became increasingly sediment-charged and pore-fluid overpressure probably developed as a result of rapid sedimentation and a decrease in overburden pressure.

6 Two of six mass-wasting events (7800 and 4900 cal yr BP) are characterized by multiple simultaneous slides (nine slides during each event), suggesting that palaeoearthquakes are a common trigger mechanism.

7 Following the lowstand around 6800 cal yr BP, lake level rose in a stepwise fashion, resulting in 11 well-preserved palaeoshorelines that are stacked vertically and laterally and dated using core-to-seismic correlation of a core taken on the northern lake shoulder. Similar to marine coastal sequences, periods of transgression with back-stepping shoreline position can be discerned from phases of regression, during which shorelines step out and down towards the lake centre. Such regressional phases that interrupt the general transgressive trend can be identified from ~5800 to 5400 and from ~4700 to 4000 cal yr BP.

8 The strengthening of the Southern Hemisphere Westerlies reached a threshold value that was strong enough to nucleate intense lake circulation around ~6000 cal yr BP. These currents led to dome-shaped sediment drifts in the northern and southern basinal areas, whereas the east–west central basin axis became sediment-starved.

ACKNOWLEDGEMENTS

We are grateful to Capitan Jorge and Javier Moreteau and their crew who transported the Catamaran *RV/Cardiel* from far north to launch it on Laguna Potrok Aike, making this study possible. We also thank the members of the INTA field station, in particular Guillermo Clifton, José Larrosa and Gabriel Oliva for providing the operational headquarters at the lake shore. Felix Bussmann and Eliane Tresch helped during acquisition of the single-channel airgun data. Francois Charlet, Koen DeRycker, Hugo Corbella and Santiago Palamedi supported the sparker data acquisition. Christoph Mayr and Michael Wille helped during the coring operations. This study was supported by the German Federal Ministry of Education and Research in the framework of the German Climate Research Program (DEKLIM; grant 01 LD 0034: project SALSA), through the project POTROK within the Priority Program 'ICDP-Germany' of the German Research Council (DFG: ZO 102/5–1, 2, 3) and by the Swiss National Science Foundation.

REFERENCES

Adams, K.D. and **Wesnousky, S.G.** (1998) Shoreline processes and the age of the Lake Lahontan highstand in the Jessup Embayment, Nevada. *GSA Bull.*, **110,** 505–524.

Anselmetti, F.S., Ariztegui, D., Hodell, D.A., Hillesheim, M., Brenner, M., Gilli, A., McKenzie, J.A. and **Mueller, A.D.** (2006) Late Quaternary climate-induced lake level variations in Lake Petén Itzá, Guatemala, inferred from seismic stratigraphic analysis. *Palaeogeogr. Palaeoclimatol. Palaeoecol.*, **230,** 52–69.

Ariztegui, D., Bianchi, M.M., Massaferro, J., Lafargue, E. and **Niessen, F.** (1997) Interhemispheric synchrony of Late-glacial climatic instability as recorded in proglacial Lake Mascardi, Argentina. *J. Quatern. Sci.*, **12,** 333–338.

Ariztegui, D., Anselmetti, F.S., Seltzer, G., Kelts, K. and **D'Agostino, K.** (2000) Identifying paleoenvironmental change across South and North America using high-resolution seismic stratigraphy in lakes. In: *Interhemispheric Climate Linkages: Present and Past Interhemispheric Climate Linkages in the Americas and their Societal Effects* (Ed. V. Markgraf), pp. 227–240. Academic Press.

Ariztegui, D., Anselmetti, F.S., Gilli, A. and **Waldmann, N.** (in press) Late Pleistocene environmental changes in Patagonia and Tierra del Fuego – a limnogeological approach. In: *Late Cenozoic of Patagonia and Tierra del Fuego* (Ed. J. Rabassa), Elsevier, in press.

Balch, D.P., Cohen, A.S., Schnurrenberger, D.W., Haskell, B.J., Valero Garces, B.L., Beck, J.W., Cheng, H. and **Edwards, R.L.** (2005) Ecosystem and paleohydrological response to quaternary climate change in The Bonneville Basin, Utah. *Palaeogeogr. Palaeoclimatol. Palaeoecol.*, **221,** 99–122.

Bard, E., Rostek, F. and **Sonzogni, C.** (1997) Interhemispheric synchrony of the last deglaciation inferred from alkenone palaeothermometry. *Nature*, **385,** 707–710.

Baruth, B., Endlicher, W. and **Hoppe, P.** (1998) Climate and desertification processes in Patagonia. *Bamberger Geographische Schriften*, **15,** 307–320.

Brooks, K., Scholz, C.A., King, J.W., Peck, J., Overpeck, J.T., Russell, J.M. and **Amoako, P.Y.O.** (2005) Late-Quaternary lowstands of Lake Bosumtwi, Ghana: evidence from high-resolution seismic reflection and sediment-core data. *Palaeogeogr. Palaeoclimatol. Palaeoecol.*, **216,** 235–249.

Chapron, E., Beck, C., Pourchet, M. and **Deconinck, J.-F.** (1999) 1822 earthquake-triggered homogenite in Lake Le Bourget (NW Alps). *Terra Nova*, **11,** 86–92.

Endlicher, W. (1993) Klimatische Aspekte zur Weidedegradation in Ost-Patagonien, In: *Beiträge zur Kultur und Regionalgeographie, Festschrift für Ralph Jätzold* (Eds B. Hornetz and D. Zimmer), *Trierer Geographische Studien*, **9,** Geographische Gesellschaft Trier, Germany, 91–103.

Gilli, A., Anselmetti, F.S., Ariztegui, D., Bradbury, J.P., Kelts, K., Markgraf, V. and **McKenzie, J.A.** (2001) Tracking abrupt climate change in the Southern Hemisphere: a seismic stratigraphic study of Lago Cardiel, Argentina (49°S). *Terra Nova*, **13,** 443–448.

Gilli, A., Anselmetti, F.S., Ariztegui, D., Beres, M., McKenzie, J.A. and **Markgraf, V.** (2005a) Seismic stratigraphy, buried beach ridges and contourite drifts: the Late Quaternary history of the closed Lago Cardiel basin, Argentina (49°S). *Sedimentology*, **51,** 1–23.

Gilli, A., Ariztegui, D., Anselmetti, F.S., McKenzie, J.A., Markgraf, V., Hajdas, I. and **McCulloch, R.D.** (2005b) Mid-Holocene strengthening of the southern westerlies in South America – sedimentological evidences from Lago Cardiel, Argentina (49ºS). *Global Planet. Change*, **49,** 75–93.

Haberzettl, T., Fey, M., Lücke, A., Maidana, N., Mayr, C., Ohlendorf, C., Schäbitz, F., Schleser, G.H., Wille, M. and **Zolitschka, B.** (2005) Climatically induced lake level changes during the last two millennia as reflected in sediments of Laguna Potrok Aike, southern Patagonia (Santa Cruz, Argentina). *J. Paleolimnol.*, **33,** 283–302.

Haberzettl, T., Wille, M., Fey, M., Janssen, S., Lücke, A., Mayr, C., Ohlendorf, C., Schäbitz, F., Schleser, G. and **Zolitschka, B.** (2006) Environmental change and fire history of southern Patagonia (Argentina) during the last five centuries. *Quatern. Int.*, **158,** 72–82.

Haberzettl, T., Corbella, H., Fey, M., Janssen, S., Lücke, A., Mayr, C., Ohlendorf, C., Schäbitz, F., Schleser, G., Wille, M., Wulf, S. and **Zolitschka, B.** (2007) Late glacial and Holocene wet-dry cycles in southern Patagonia: chronology, sedimentology and geochemistry of a lacustrine record from Laguna Potrok Aike, Argentina. *The Holocene*, **17,** 297–311.

Haberzettl, T., Kück, B., Wulf, S., Anselmetti, F.S., Ariztegui, D., Corbella, H., Fey, M., Janssen, S., Lücke, A., Mayr, C., Ohlendorf, C., Schäbitz, F., Schleser, G., Wille, M. and **Zolitschka, B.** (2008) Hydrological variability in southeastern Patagonia and explosive volcanic activity in the southern Andean Cordillera during Oxygen Isotope Stage 3 and the Holocene inferred from lake sediments of Laguna Potrok Aike, Argentina. *Palaeogeogr. Palaeoclimatol. Palaeoecol.*, **259,** 213–229.

Hampton, M.A., Lee, H.J. and **Locat, J.** (1996) Submarine landslides. *Rev. Geophys.*, **34,** 33–59.

Heusser, C.J. (1995) Three late Quaternary pollen diagrams from Southern Patagonia and their palaeoecological implications. *Palaeogeogr. Palaeoclimatol. Palaeoecol.*, **118,** 1–24.

Hunt, D. and **Tucker, M.E.** (1992) Stranded parasequences and the forced regressive wedge systems tract: deposition during base-level fall. *Sed. Geol.*, **81,** 1.

Ibbeken, H. and **Warnke, D.A.** (2000) The Hanaupah-Fan shoreline deposit at Tule Spring, a gravelly shoreline deposit of Pleistocene Lake Manly, Death Valley, California, USA. *J. Paleolimnol.*, **23,** 439–447.

Komatsu, G., Brantingham, P.J., Olsen, J.W. and **Baker, V.R.** (2001) Paleoshoreline geomorphology of Boon Tsagan Nuur, Tsagaan Nuur and orog Nuur, the Valley of Lakes, Mongolia. *Geomorphology*, **39,** 83–98.

Lamy, F., Hebbeln, D., Röhl, U. and **Wefer, G.** (2001) Holocene rainfall variability in southern Chile: a marine record of latitudinal shifts of the Southern Westerlies. *Earth Planet. Sci. Lett.*, **185,** 369–382.

Lamy, F., Rühlemann, C., Hebbeln, D. and **Wefer, G.** (2002) High- and low-latitude climate control on the position of the southern Peru-Chile Current during the Holocene. *Paleoceanography*, **17,** 1029/2001PA000727.

Locat, J. and **Lee, H.J.** (2002) Submarine landslides: advances and challenges. *Can. Geotech. J.*, **39,** 193–212.

Marengo, J. and **Rogers, J.** (2001) Polar air outbreaks in the Americas: assessments and impacts during modern and past climates. In: *Interhemispheric Climate Linkages* (Ed. V. Markgraf), pp. 31–51. Academic Press, San Diego, CA.

Markgraf, V. (1993) Climatic history of Central and South America since 18,000 years B.P.: comparison of pollen records and model simulations. In: *Global Climates since the Last Glacial Maximum* (Eds H.E. Wright, J.E. Kutzbach, T. Webb, III, W.F. Ruddiman, F.A. Street-Perrott and P.J. Bartlein), pp. 357–385. University of Minnesota Press, Minneapolis, MN; London.

Markgraf, V., Baumgartner, T.R., Bradbury, J.P., Diaz, H.F., Dunbar, R.B., Luckman, B.H., Seltzer, G.O., Swethnam, T.W. and **Villalba, R.** (2000) Paleoclimate reconstruction along the Pole-Equator-Pole transect of the Americas (PEP 1). *Quatern. Sci. Rev.*, **19,** 125–140.

Markgraf, V., Bradbury, J.P., Schwalb, A., Burns, S., Stern, C., Ariztegui, D., Gilli, D., Anselmetti, F.S., Stine, S. and **Maidana, N.** (2003) Holocene paleoclimate of Southern Patagonia: Limnological and environmental history of Lago Cardiel, Argentina. *The Holocene*, **13,** 581–591.

Mayr, C., Wille, M., Haberzettl, T., Fey, M., Janssen, S., Lücke, A., Ohlendorf, C., Oliva, G., Schäbitz, F., Schleser, G. and **Zolitschka, B.** (2007) Holocene variability of the Southern Hemisphere westerlies in Argentinean Patagonia (52°S). *Quatern. Sci. Rev.*, **26,** 579–584.

Moernaut, J., De Batist, M., Charlet, F., Heirman, K., Chapron, E., Pino, M., Brümmer, R. and **Urrutia, R.** (2006) Giant earthquakes in South-Central Chile revealed by Holocene mass-wasting events in Lake Puyehue. *Sed. Geol.*, **195,** 239–256.

Monecke, K., Anselmetti, F.S., Becker, A., Sturm, M. and **Giardini, D.** (2004) The record of historic earthquakes in lake sediments of Central Switzerland. *Tectonophysics*, **394,** 21–40.

Plint, A.G. and **Nummedal, D.** (2000) The falling stage systems tract: recognition and importance in sequence stratigraphic analysis. In: *Sedimentary Response to Forced Regression* (Eds D. Hunt and R.L. Gawthorpe), *Geol. Soc. London Spec. Publ.*, **172,** 1–17.

Posamentier, H.W. and **Allen, G.P.** (1999) Siliciclastic sequence stratigraphy: concepts and applications. *SEPM Concepts Sedimentol. Paleontol.*, **7,** 210.

Rabineau, M., Berné, S., Olivet, J.L., Aslanian, D., Guillocheau, F. and **Joseph, P.** (2006) Paleo sea levels reconsidered from direct observation of paleoshoreline position during Glacial Maxima (for the last 500,000 yr). *Earth Planet. Sci. Lett.*, **252,** 119–137.

Reimer, P.J., Baillie, M.G.L., Bard, E., Bayliss, A., Beck, J.W., Bertrand, C., Blackwell, P.G., Buck, C.E., Burr, G., Cutler, K.B., Damon, P.E., Edwards, R.L., Fairbanks, R.G., Friedrich, M., Guilderson, T.P., Hughen, K.A., Kromer, B., McCormac, F.G., Manning, S., Bronk Ramsey, C., Reimer, R.W., Remmele, S., Southon, J.R., Stuiver, M., Talamo, S., Taylor, F.W., van der Pflicht, J. and **Weyhenmeyer, C.E.** (2004) IntCal04 Terrestrial radiocarbon age calibration, 26–0 ka BP. *Radiocarbon*, **46,** 1029–1058.

Schnellmann, M., Anselmetti, F.S., Giardini, D., McKenzie, J.A. and **Ward, S.** (2002) Prehistoric earthquake history revealed by lacustrine slump deposits. *Geology*, **30,** 1131–1134.

Schnellmann, M., Anselmetti, F.S., Giardini, D. and **McKenzie, J.A.** (2005) Mass movement-induced fold-and-trust belt structures in unconsolidated sediments in Lake Lucerne. *Sedimentology*, **52,** 271–289.

Seltzer, G.O., Baker, P., Cross, S., Dunbar, R. and **Fritz, S.** (1998) High-resolution seismic reflection profiles from Lake Titicaca, Peru-Bolivia: Evidence for Holocene aridity in the tropical Andes. *Geology*, **26,** 167–170.

Strasser, M., Anselmetti, F.S., Fäh, D., Giardini, D. and **Schnellmann, M.** (2006) Magnitudes and source areas of large prehistoric northern Alpine earthquakes revealed by slope failures in lakes. *Geology*, **34,** 1005–1008.

Strasser, M., Stegmann, S., Bussmann, F., Anselmetti, F.S., Rick, B. and **Kopf, A.** (2007) Quantifying subaqueous slope stability during seismic shaking: Lake Lucerne as model for ocean margins. *Mar. Geol.*, **240,** 77–97.

Stuiver, M. and **Reimer, P.** (1993) Extended 14C database and revised CALIB radiocarbon calibration program. *Radiocarbon*, **35,** 215–230.

Stuiver, M., Reimer, P. and **Reimer, R.** (2005) *Calib 5.0* (WWW program and documentation). http://calib.qub.ac.uk/calib.

Sultan, N., Cochonat, P., Canals, M., Cattaneo, A., Dennielou, B., Haflidason, H., Laberg, J.S., Long, D., Mienert, J. and **Trincardi, F.** (2004) Triggering mechanisms of slope instability processes and sediment failures on continental margins: a geotechnical approach. *Mar. Geol.*, **213,** 291–321.

Thompson, T.A. (1992) Beach-ridge development and lake level variation in southern Lake Michigan. *Sed. Geol.*, **80,** 305–318.

Thompson, L.G., Mosley-Thompson, E. and **Henderson, K.A.** (2000) Ice-core palaeoclimate records in tropical South America since the Last Glacial Maximum. *J. Quatern. Sci.*, **15,** 377–394.

Vail, P.R., Mitchum, R.M. and **Thompson III, S.** (1977) Cycles of relative changes of sea level. In: *Seismic Stratigraphy—Applications to Hydrocarbon Exploration* (Ed. C.E. Payton), *AAPG Mem.*, **26,** 83–97.

Waldmann, N., Ariztegui, D., Anselmetti, F.S., Austin Jr, J.A., Dunbar, R.M., Moy, C.M. and **Recasens, C.** (2008) Seismic stratigraphy of Lago Fagnano sediments (Tierra del Fuego, Argentina) – a potential archive of paleoclimatic change and tectonic activity since the Late Glacial. *Geol. Acta*, **6,** 101–110.

Wille, M., Maidana, N.I., Schäbitz, F., Fey, M., Haberzettl, T., Janssen, S., Lücke, A., Mayr, C., Ohlendorf, C., Schleser, G.H. and **Zolitschka, B.** (2007) Vegetation and climate dynamics in southern South America: the microfossil record of Laguna Potrok Aike, Santa Cruz, Argentina. *Rev. Palaeobot. Palynol.*, **146,** 234–246.

Zolitschka, B., Schäbitz, F., Lücke, A., Corbella, H., Ercolano, B., Fey, M., Haberzettl, T., Janssen, S., Maidana, N., Mayr, C., Ohlendorf, C., Oliva, G., Paez, M., Schleser, G.H., Soto, J., Tiberi, P. and **Wille, M.** (2006) Crater lakes of the Pali Aike Volcanic Field as key sites for paleoclimatic and paleoecological reconstructions in southern Patagonia, Argentina. *J. S. Am. Earth Sci.*, **21,** 294–309.

Manuscript received 30 December 2007; revision accepted 23 July 2008